

OneVAE: Joint Discrete and Continuous Optimization Helps Discrete Video VAE Train Better

Yupeng Zhou^{1,2}, Zhen Li³, Ziheng Ouyang¹, Yuming Chen¹, Ruoyi Du², Daquan Zhou⁴, Bin Fu², Yihao Liu², Peng Gao², Ming-Ming Cheng¹, Qibin Hou^{†1}

¹VCIP, School of Computer Science, Nankai University

²Shanghai AI Laboratory

³The Chinese University of Hong Kong

⁴Peking University

[†]Corresponding author

Abstract: Encoding videos into discrete tokens could align with text tokens to facilitate concise and unified multi-modal LLMs, yet introducing significant spatiotemporal compression compared to continuous video representation. Previous discrete video VAEs experienced unstable training, long training time, and degraded reconstruction quality. Given the easier training and superior performance of continuous VAEs, an intuitive idea is to enhance discrete video VAEs by leveraging continuous VAEs. After rethinking the intrinsic link between discrete and continuous representations, we found that FSQ could effectively preserve pre-trained continuous VAE priors compared to other quantization methods. By leveraging continuous VAE priors, it converges several times faster than training from scratch and achieves superior performance at convergence. Meanwhile, two structural improvements are proposed. First, inspired by how continuous VAEs enhance reconstruction via enlarged latent dimensions, we introduce a multi-token quantization mechanism, which achieves nearly a 1 dB improvement in PSNR without compromising the token compression ratio. Second, to tackle reconstruction challenges in high-compression video VAEs, we strengthen first-frame reconstruction, enabling the causal VAE to leverage this information in subsequent frames and markedly improving the performance of $4 \times 16 \times 16$ discrete VAEs. Furthermore, we propose a joint discrete–continuous optimization scheme that unifies the two paradigms and, for the first time, achieves competitive performance on both continuous and discrete representations within a single network. We name our method OneVAE to reflect this connection.

Code: <https://github.com/HVision-NKU/OneVAE>

HVision@Nankai

1 Introduction

Auto-regressive language LLMs have shown strong performance, sparking interest in extending their capabilities to image and video generation. In particular, a series of autoregressive generative models [46, 55, 38] have already achieved impressive results in this direction. A key challenge in extending these models to visual domains is that raw visual data (e.g., RGB pixels) is far more complex than plain text, which raises issues in how to represent such visual content into tokens. Looking back at diffusion-based generation works, the pioneering work Stable Diffusion [34] succeeded in introducing continuous VAE to enable the generation of photorealistic images with limited computational

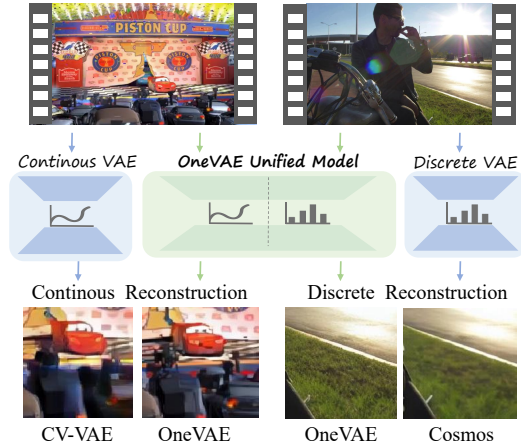


Figure 1 Illustration of OneVAE, which could encode both discrete and continuous representations, distinguishing from traditional discrete-only [29] and continuous-only [57] VAEs.

resources. Since then, the field of AIGC research has advanced rapidly, with a series of generative models [6, 10, 30, 52, 20, 27] providing more powerful visual generation results. However, continuous representations do not align well with LLMs for pure next-token prediction, as it is difficult to directly predict continuous tokens [23].

Previous auto-regress generative models [38, 9, 40] introduced discrete VQ-VAEs [11] to encode visual content, align them with text tokens, and allow a unified autoregressive next-token prediction architecture. Despite these impressive results, the VQ-VAEs employed in previous work face two key limitations. First, due to the heightened difficulty in balancing compression efficiency and information preservation in discrete representations compared to continuous ones, their reconstruction quality still leaves room for enhancement. Second, as these works have only focused on image generation, their VQ-VAEs are confined to encoding images alone.

Compared to their image-based counterparts, discrete video VAEs must additionally compress temporal dimension information, rendering the design of a robust discrete video VAE far more demanding. In the early exploration of discrete video VAE, most works also relied on VQ-based quantization: VideoGPT [51] adopted a relatively low compression ratio of $4 \times 4 \times 4$ to preserve performance, while OmniTokenizer [45] introduced a hybrid image-video encoder using $4 \times 8 \times 8$ configuration. EMU-3 [46] further improved the reconstruction quality of the VQ-VAE. Due to the inherent training instability of VQ, the Cosmo Tokenizer [29] incorporated the quantization of FSQ [28] into its VAE architecture. Using FSQ’s improved stability, it was able to support multiple VAEs with varying compression ratios. Although significantly improving the reconstruction performance of discrete VAEs, the discrete Cosmos Tokenizers still lag behind their continuous counterparts.

This discrepancy motivates us to further explore ways to enhance the performance of discrete VAEs in this paper. We first engaged in rethinking the distinctions between continuous and discrete encoding. For current discrete tokenizers, video sequences are compressed into continuous features, and different quantization methods are employed to quantize these continuous features. Based on how the features are processed, we categorize the quantization methods into two types: (1) codebook lookup-based ones, which aim to find the vector with the closest distance in the codebook; (2) rounding operation-based ones, which directly round on the mapped features. Unlike VQ [11], which uses codebook distance, FSQ [28] maps continuous features into a bounded range and rounds them, making it closer to continuous encoding. We verified this by training a lightweight quantizer in the latent space of continuous VAEs, optimizing only its parameters. As shown in Tab. 2, FSQ outperforms VQ (PSNR 26.46 vs. 22.82). This confirms FSQ’s closer relation to continuous VAEs and suggests continuous VAEs can support discrete ones, opposing the view that they are independent training [29].

Based on these observations, we propose a progressive training strategy to accelerate convergence. We start with an $8 \times 8 \times 4$ continuous tokenizer, then expand to an $8 \times 8 \times 4$ discrete tokenizer and a $16 \times 16 \times 4$ continuous tokenizer, and finally transition to a $16 \times 16 \times 4$ discrete tokenizer. We choose pretrained VAEs [20, 43] as the starting point for training, as such models are typically trained on large non-public higher-quality datasets. Our goal is for the progressive pipeline to preserve these useful priors. As shown in Fig. 5, unlike methods such as Cosmos Tokenizer [29] that train separate continuous and discrete tokenizers from scratch, our progressive approach achieves competitive performance with significantly fewer training iterations, greatly accelerating training. Moreover, the experimental results support that our model achieves better reconstruction performance. Building on this, we further propose an ambitious idea: Could a single model simultaneously learn both discrete and continuous representations? To explore this, we propose a dual-path joint optimization strategy, which includes an additional FSQ-based discretization branch and a continuous branch, allowing the model to encode both continuous and discrete data during training. The experimental results give a clear confirmation. Our unified model can effectively handle both representations, and ablation studies show that it even improves certain metrics, further demonstrating their intrinsic connection and mutual reinforcement.

We also introduce meaningful structural enhancements, including multi-token quantization, first-frame enhancement for causal VAEs, and decoder expansion, to improve performance under high compression ratios. Multi-token quantization alleviates codebook size constraints by encoding each feature position into multiple tokens (two in our experiments). The first frame enhancement stems from our observation that, in causal VAEs, the first frame often suffers from lower quality than subsequent frames due to limited accessible information. By reducing the compression ratio of the first frame only, we significantly improve reconstruction quality for both the first and subsequent frames. Finally, decoder expansion enhance reconstruction capacity by increasing the model’s parameters. Together, these modifications lead to substantial performance gains.

Our contributions are summarized as follows:

- We propose a progressive training strategy that transitions from a pretrained continuous VAE to discrete VAEs, effectively leveraging prior knowledge to accelerate convergence.
- We introduce structural enhancements including multi-token quantization and first-frame enhancement for causal VAEs, both of which substantially improve reconstruction quality.
- We develop a unified tokenizer that jointly models discrete and continuous representations, achieving superior reconstruction performance for both.

2 Relate Work

2.1 Generation Model

Generative models have demonstrated remarkable performance across various domains. In the early stages, Generative Adversarial Networks (GANs) [13, 18, 3] emerged as one of the pioneering and most influential visual generation methods in the deep learning era. Recently, diffusion models [14] have demonstrated unprecedented performance in generative tasks, notably in the domain of text-to-image synthesis [32, 34, 35], through a systematic noise removal process. Subsequent advancements extended diffusion-based methodologies to video generation. Some video diffusion models directly model pixel-value distributions [22, 37], while others concentrate on modeling the distributions of latent tokens, typically extracted using Variational Autoencoders (VAEs) [2, 44], rather than directly handling pixel data. As an alternative technical approach, autoregressive models [11, 33, 53] are a class of generative models widely used to predict the next token in a sequence, inspired by GPT-style [31] architectures. To reduce computational cost and enhance the quality of generated outputs, these methods rely on discrete or continuous VAEs, leveraging their ability to perform compression-based high-fidelity reconstruction.

2.2 Discrete VAEs

Recent advancements in video generation have been significantly involved with the auto-regressive models, driven by the rising popularity of large language models. This approach requires a discrete tokenizer to quantize visual information by mapping input images into a latent space and identifying the nearest codebook vectors. Notable models such as TATS [12], MAGVIT [54], and VideoGPT [51] leverage discrete token training within the VQVAE [42] framework, employing 3D VAEs to extract discrete tokens. TATS [12], for example, introduces a hierarchical sampling strategy with autoregressive and interpolation Transformers, improving both generation quality and efficiency. MAGVIT-v2 [55] refines the VQ-VAE codebook by reducing its embedding dimension to zero and incorporating Lookup-Free Quantization (LFQ), which has been widely adopted in contemporary models. VideoGPT [51] utilizes VQ-VAE, applying 3D convolutions and axial self-attention to learn downsampled discrete latent representations of video data. Additionally, newer models, such as LaViT [17] and ElasticTok [50], generate dynamic discrete visual tokens while preserving high-level semantic information. Approaches like the Omni-tokenizer [45], a joint image and video tokenizer, and Cosmos-Tokenizer [29], which uses Finite Scalar Quantization, further enhance the discrete tokenization process. At the same time, different improvements for discretization methods have been proposed in combination with diverse model architectures, such as VQ [11], LFQ [55], CVQ [58], IBQ [36], and FSQ [28]. These strategies optimize the tokenization process, significantly contributing to advancements in visual generation. Among these studies, CVQ alleviates code collapse by learning the cluster codebook. LFQ improves upon the original VQ by eliminating the lookup step. IBQ improves the discretization process by modifying the gradient calculation method for optimizing the codebook training. and FSQ simplifies quantization by using a fixed mapping and rounding operation, improving stability.

2.3 Continuous VAE

Compared to discrete tokenization, continuous tokenization [57, 7, 39, 52] typically offers higher reconstruction fidelity. In the field of image generation, Stable Diffusion [34] introduced the use of continuous VAEs in diffusion models, significantly enhancing image generation. This approach has inspired numerous subsequent works [6, 10, 30] in the field of video generation. Some studies integrate 3D convolutions or spatio-temporal

attention mechanisms into the backbone network [1, 15, 37, 49, 16], creating latent spaces specifically designed for video data. Video generation models initially performed frame-by-frame decoding, but following Sora [4], a series of video diffusion models trained video VAEs to compress data along the temporal dimension [20, 24, 59, 21, 52]. Some works like Hunyuan Video [20] and Allegro VAE [24] also contributed to this paradigm shift. OpenSora [59] and OpenSoraPlan [21] are open-source projects aimed at replicating OpenAI’s Sora, offering efficient continuous VAEs. Meanwhile, CogVideoX [52] retains more information by preserving a larger number of latent channels. Additionally, Cosmos-Tokenizer [29] provides a suite of continuous video tokenizers with various compression ratios. CV-VAE [57] employs latent space regularization to align the video latent space with the latent space of existing image VAEs [34], enabling effective spatio-temporal compression. In contrast to previous approaches that handle discrete and continuous representations in isolation, we introduce OneVAE, which unifies both types within a single framework. By combining progressive training strategies and architectural modifications, our method achieves improved reconstruction quality for discrete representations while maintaining strong performance across representation types.

3 Method

3.1 Preliminaries of Continuous and Discrete VAEs

Continuous and discrete VAEs differ fundamentally in how they represent latent variables. Continuous VAEs [19] model the latent space as a continuous probability distribution, where the encoder $E(x)$ maps the input x to the parameters of a distribution—typically a Gaussian. The latent variable z is then sampled from this distribution.

$$E(x) = \mathcal{N}(\mu, \sigma^2), \quad z \sim E(x) \quad (1)$$

where $\mathcal{N}(\mu, \sigma^2)$ represents a Gaussian distribution with mean μ and variance σ^2 .

Same as continuous VAEs, discrete VAEs compress video data $V \in \mathbb{R}^{C \times T \times H \times W}$ into a low-resolution representation $z \in \mathbb{R}^{D \times \frac{T}{t} \times \frac{H}{h} \times \frac{W}{w}}$ through the encoder and then decompress back to the original representation \hat{x} using the decoder:

$$z = E(x), \quad \hat{x} = D(z) \quad (2)$$

where $E(\cdot)$ represents the encoder and $D(\cdot)$ is the decoder. Discrete VAEs [36, 11] typically remove the Gaussian sampling process used in continuous VAEs. To convert z into a discrete token, two primary quantization strategies exist. VQ-based quantization selects the closest vector from a predefined codebook $\mathcal{C} = \{c_i\}_{i=1}^N$ based on Euclidean distance:

$$q_i = \arg \min_{c_i \in \mathcal{C}} \|z_i - c_i\|_2. \quad (3)$$

Alternatively, FSQ-based quantization [28] directly constrains each dimension of z within a bounded range and applies a rounding operation:

$$q_i = \text{Round}(\text{Bound}(z_i)). \quad (4)$$

After that, the d dimensions of q_i are all integers in $(-L/2, L/2)$, and they can be easily converted into an index.

Intuitively, the FSQ-based approach involves only a simple mapping and rounding of continuous features, which makes it highly similar to those features. To explore this, we experiment in Tab. 2 by training quantizer modules based on FSQ and VQ into a pre-trained continuous VAE to train using discrete reconstruction loss. The results show that FSQ outperforms VQ, suggesting that the discrete features encoded by FSQ exhibit a higher similarity to the continuous features of the VAE.

Quant. Method	PSNR \uparrow	SSIM \uparrow	LPIPS \downarrow
FSQ	26.46	0.8566	0.0825
VQ	22.82	0.7310	0.2071

Figure 2 Comparison of VQ [11] and FSQ [28] trained in the latent space of a continuous VAE, where only the intermediate quantization modules are trained.

3.2 Improved Training Procedure and Structure

Tree-Structured Progressive Training. VAEs are traditionally trained separately. To accommodate different compression ratios, both discrete and continuous VAEs may need to be trained as a suite of multiple models,

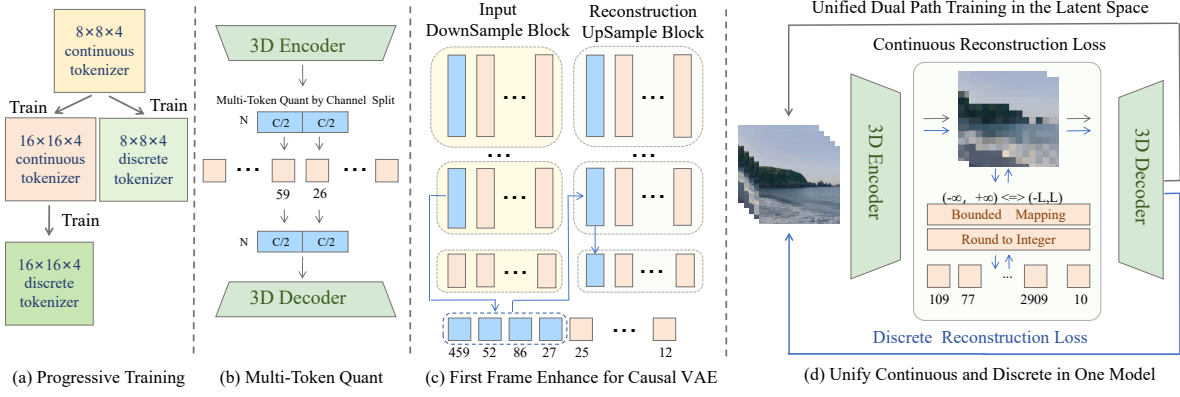


Figure 3 Training method and architecture of the proposed model. Figure (a) illustrates the progressive training process, where all models are derived from an $8 \times 8 \times 4$ continuous VAE, which can be either the HunyuanVideo VAE [20] or the Wan VAE [43] to provide pre-trained data priors. Figure (b) demonstrates the working principle of multi-token quantization, which can significantly enhance the representational capacity. Figure (c) illustrates the First-Frame Enhancement mechanism: by reducing the compression strength of the first frame to strengthen its reconstruction, it enables the causal VAE to leverage this information in subsequent frames, markedly improving the $4 \times 16 \times 16$ discrete encoder’s reconstruction quality. Figure (d) presents the unified training framework that integrates both continuous and discrete paths in the latent space. In the continuous path, the 3D encoder maps the input data to a continuous latent representation ($C \times T \times H \times W$), which is optimized by the continuous reconstruction loss. In the discrete path, after bounded mapping and integer rounding, the FSQ quantization method converts the continuous latent representation into discrete tokens ($C \times T \times H \times W \rightarrow N$ Token), which are trained with the discrete reconstruction loss. This approach enables the model to handle continuous and discrete data simultaneously with better performance for both.

leading to significant computational overhead. Moreover, as shown in the training details of Open-SORA [59] and Open-SORA-Plan [25], video VAEs often require extended training times. Additionally, compared to continuous VAEs, discrete VAEs suffer significant information loss due to the quantization process and are prone to issues such as code collapse [11], making training increasingly challenging. Based on the analysis presented in Sec. 3.1 and the experimental results in Tab. 2, we argue that continuous VAEs can serve as an effective warm-up for training discrete VAEs. The key insight is to leverage the latent space representations learned by the continuous VAE to facilitate the training of the discrete VAE. This approach allows the model to start training from a well-optimized state rather than from random initializations. In our training pattern, we first train a $8 \times 8 \times 4$ continuous VAE and then gradually extend it to both discrete and continuous VAEs with $8 \times 8 \times 4$ and $16 \times 16 \times 4$ configurations. For converting the continuous VAE to a discrete VAE, we simply insert an FSQ quantization module into the middle of the pre-trained continuous VAE to discretize it into tokens. Afterward, we fine-tune the model to optimize it for discrete representations. To further minimize discrepancies, we initialize the discrete VAE from a continuous VAE with the same downsampling ratio. Therefore, for high-compression discrete VAEs, we first obtain a high-compression continuous VAE through progressive training and then convert it into a discrete VAE using the same approach. As shown in Fig. 3(a), we refer to this approach as tree-structured progressive training, where all models are derived from a $8 \times 8 \times 4$ continuous VAE. By adopting this progressive training strategy, we ensure that the training process remains manageable, allowing the model to learn effectively at each stage before advancing to the next level of complexity.

Multi-Token Quantization As illustrated in Fig. 3 (b), we propose a multi-token quantization strategy that decomposes each latent feature vector along its channel dimension into multiple smaller sub-vectors, and quantizes each independently. Specifically, each feature channel is divided into several segments—for example, two equal parts in our implementation. Each segment is then quantized separately into discrete tokens using shared codebooks. This approach increases the effective representational capacity without enlarging the total codebook size, as multiple tokens collectively encode the original vector with finer granularity. By capturing more subtle variations within each channel, multi-token quantization enables a richer and more flexible discrete representation of latent features. As a result, this leads to improved reconstruction fidelity and overall performance. Compared to conventional single-token quantization that compresses an entire channel vector into one token, our method strikes a balance between compression and expressiveness, addressing the limited expressiveness of traditional vector quantization methods under high compression ratios. This design constitutes a key contribution

of our work, demonstrating substantial performance improvement.

First-Frame Enhancement Previous works on causal VAEs [29, 47, 39] have either explicitly noted or been implicitly observed (e.g., in open-source model outputs) that high compression video VAE tend to degrade the quality of early frames in a sequence. However, this issue has not been effectively addressed. By comparing the same VAE architecture under causal and non-causal settings in Fig. 4, we found that the inferior quality of early frames in the causal setting likely stems from their limited accessible information. As illustrated in Fig. 3(c), we propose a *First-Frame Enhancement* strategy to address this issue. The key idea is to reduce the compression strength of the first frame by allocating more tokens per spatial unit, while keeping the overall video compression ratio unchanged. This design enriches the structural and textural fidelity of the anchor frame, which in turn serves as a higher-quality reference for reconstructing subsequent frames in a causal manner. As shown in Fig. 4, compared to uniform high-ratio compression, which can severely degrade early-frame details and disrupt temporal consistency, our method preserves anchor-frame fidelity without increasing the token budget. This targeted adjustment significantly improves both the first-frame reconstruction and the temporal coherence of later frames, leading to substantial performance gains in high-compression discrete VAE.

Expanding Decoder. In high-compression discrete VAEs, quantization leads to a significant reduction in the amount of information retained in the latent space, which directly impacts the quality of the output. Therefore, the original decoder faces a challenge, as it must compensate for this loss while generating meaningful and coherent results, which is responsible for reconstructing the data. We argue that the reconstruction module needs to be larger to effectively handle the associated complexities. When training the $16 \times 16 \times 4$ discrete VAE, we insert additional layers into the decoder to improve reconstruction quality. As shown in Tab. 6, by scaling the decoder, we provide it with more expressive power, enabling it to better reconstruct the data despite the challenges posed by discretization, which leads to a noticeable improvement in reconstruction performance.

3.3 Joint Optimization For Unify VAE

Joint Discrete and Continuous Dual Path Training. Building on the improved training techniques outlined in Sec. 3.2, we introduce our OneVAE, which adopts a joint discrete and continuous optimization approach to help discrete VAE training. As show in Fig. 3(b), our method simultaneously optimizes two pathways during training: One path performs discrete reconstruction, while the other performs continuous reconstruction. Specifically, at each training step, we randomly choose whether the latent variable will be encoded discretely or continuously, and the model adjusts its encoding accordingly. The model is jointly optimized using the loss from discrete reconstruction L_d and the loss from continuous reconstruction L_c . The loss function of our joint discrete and continuous optimization is defined as follows:

$$L = \begin{cases} L_d, & \text{if } r < R_{dis} \\ L_c, & \text{if } r \geq R_{dis} \end{cases} \quad (5)$$

where R_{dis} is a ratio that controls the proportion between discrete and continuous reconstruction, and r is a random number in the range $(0, 1)$. We propose this approach for two main reasons. First, to preserve the continuous VAE prior, we introduce a tree-structured progressive training as outlined in Sec. 3.2, where we initialize a discrete VAE from a continuous VAE as a strong starting point. This joint optimization prevents the disruption of the learned continuous priors during the transition to a discrete representation, ensuring that the underlying structure learned from the continuous VAE continues to guide the training process of the discrete



Figure 4 Visual comparison illustrating our First-Frame Enhancement strategy. The second column shows results from a causal $4 \times 16 \times 16$ video VAE, where the first frame suffers from noticeably poorer reconstruction quality than subsequent frames, and the overall performance lags behind the non-causal VAE in the third column. With our First-Frame Enhancement, the fourth column shows substantial improvements in both the first and subsequent frames. Zoom in to examine text reconstruction details.

VAE. The results of the ablation experiments in Tab. 6 further validate our conclusions. Through progressive continuous initialization and the continuous-discrete joint optimization, the performance of our model can be improved compared to the baseline.

Unified Model. Through the explorations above, we discover the interplay between discrete and continuous representations and find that the continuous VAE can significantly aid in training the discrete VAE. In our original dual-path training, we introduce a ratio R_{dis} that controls the proportion between discrete and continuous reconstruction loss. A natural idea that follows is whether this dual-path joint optimization, which simultaneously incorporates both the continuous and discrete paths, can be extended to a unified model capable of simultaneously encoding both continuous and discrete representations. Since the original dual-path training is primarily designed to enhance the discrete representation, R_{dis} is set to a high value to ensure that the discrete path occupies a large proportion. To explore the unified model, we set the ratio to 0.5 to balance the proportion, which could enable a trade-off between discrete and continuous representations, and train the unified model accordingly. Surprisingly, we find that with balanced dual patch training, we obtain a unified model that performs well in both discrete and continuous encoding. Moreover, as shown in Tab. 1, our unified model achieves strong performance in both discrete and continuous representation tasks. The ability to simultaneously handle both types of representations allows the model to leverage their respective strengths, outperforming previous models in both discrete and continuous reconstruction tasks. Our unified model further proves that discrete and continuous representations are not isolated, breaking the previous notion of training them separately and providing interesting insights for future VAE research.

4 Experiments

4.1 Implementation Details

Training. Following previous work [57], we train our model on the WebVid-10M dataset. AdamW [26] optimizer is used in the training, with hyperparameters set to $\beta_1 = 0.5$ and $\beta_2 = 0.9$, following VQGAN [36]. To reduce memory overhead, we train the model using 16-bit floating-point precision (FP16). Before training, video data was preprocessed into 17-frame clips, with each frame resized to 256×256 resolution. We employed a batch size of 8 for all training iterations. We also incorporated Temporal PatchGAN [5] to enhance the model’s generative capabilities. The GAN training was initiated after a 20K-step warm-up phase, ensuring stable adversarial learning.

Evaluation. Follow pervious work [25, 57], evaluation is conducted on Panda 70M [8] at a resolution of $33 \times 512 \times 512$. We first resize the shorter side of the original video to 512, followed by a central crop. To evaluate our model, we use multiple metrics across different aspects. For reconstruction quality, we employ PSNR, SSIM [48], and LPIPS [56]. These metrics measure pixel-wise accuracy, structural similarity, and perceptual similarity, respectively. Furthermore, FVD [41] is used to assess visual quality and temporal consistency.

4.2 Ablation Study

Ablation of Progressive Training. As shown in Fig. 5, to verify the effectiveness of our progressive training strategy, we compare three training settings: (1) training from scratch using FSQ [28], (2) progressive training with SimVQ [60], and (3) progressive training with FSQ. As shown in Fig. 5, progressive training using FSQ leads to both faster convergence and better final reconstruction quality. Specifically, the progressive-FSQ strategy achieves a significant $5\times$ speed-up in convergence compared to training FSQ from scratch, reducing the number

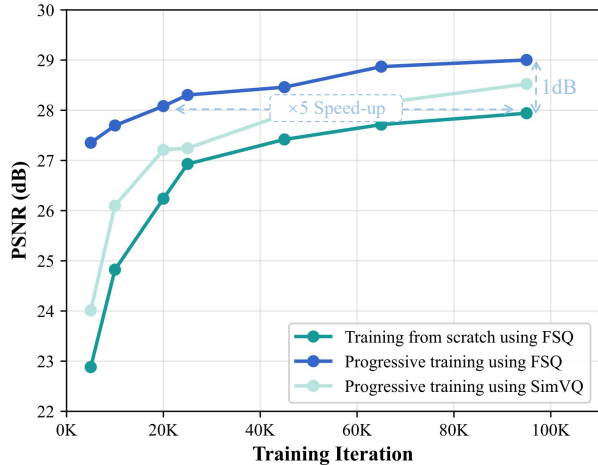


Figure 5 PSNR in training iterations for three different methods. Progressive training with FSQ achieves a significant $5\times$ convergence speedup compared to training from scratch, and attains better upper-bound performance than both progressive training with SimVQ and training FSQ from scratch.

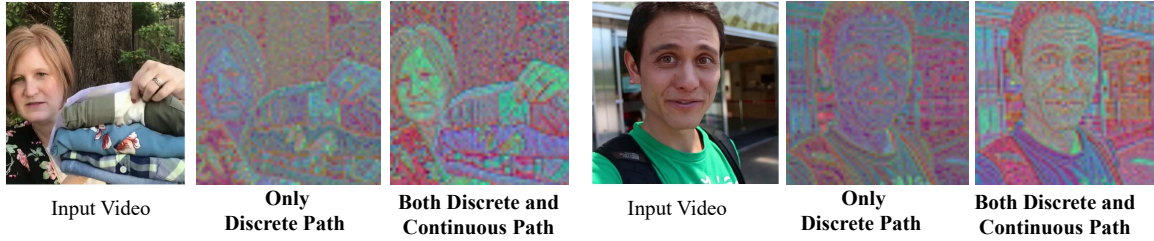


Figure 7 Visual comparison between training with only discrete path and both paths. We visualize and compare the features before quantization. Our proposed joint discrete and continuous paths training enables the model to capture richer features in the latent space for more effective video encoding.

of iterations needed to reach high-quality results. Moreover, it surpasses both baselines in final performance, attaining a PSNR improvement of approximately 1dB. Notably, progressive training with SimVQ also accelerates early convergence but saturates at a lower PSNR. We attribute the superior final performance of FSQ to its closer alignment with continuous representations, which helps retain useful priors during the transition from continuous to discrete modeling.

Latent Space Visualization. To demonstrate the effectiveness of our dual-path optimization, we visualize and compare the features before quantization between the model optimized using only the discrete path and the model optimized using both the continuous and discrete paths. As shown in the Fig. 7, training with both discrete and continuous paths enables the model to capture richer features in the latent space. We hypothesize that this improvement is due to the enhanced connection between the decoder and encoder in dual-path reconstruction. In discrete tokenizers, backpropagation relies on using the gradients of discrete vectors as approximations for continuous features by stopping gradients, which may introduce inaccuracies in gradient propagation. In contrast, our unified training approach likely helps the model achieve more precise gradient flow, leading to more effective video encoding.

Expanding the Decoder. As mentioned in Sec. 3.2, to achieve better reconstruction in high-compression ($16 \times 16 \times 4$) discrete VAEs, we increased the decoder’s capacity by adding additional layers. As shown in Tab. 6, we observed a noticeable improvement in PSNR and SSIM. The increased decoder approach resulted in a PSNR of 25.05 and an SSIM of 0.8003, compared to the baseline performance of 24.86 and 0.7950, respectively. These results suggest that expanding the decoder helps mitigate information loss at high compression ratios and improves overall performance.

Comp. Rate	Method	PSNR	SSIM
$4 \times 16 \times 16$	Baseline	24.86	0.7950
$4 \times 16 \times 16$	+ Expanding Decoder	25.05	0.8003

Figure 6 Expanding the decoder further improves the performance of $4 \times 16 \times 16$ compression VAE.

4.3 Quantitative Comparison

As shown in Tab. 1, we provide a quantitative comparison of our proposed unified model, OneVAE with several continue-only and discrete-only baseline models, including CV-VAE [57], Open-Sora [59], Open-Sora-Plan [25], OmniTokenizer[45], Cosmos Tokenizer [29] and Emu-3 [46]. Due to the $16 \times 16 \times 4$ ratio, lack of comparison models, we modified the Cosmos Tokenizer from $16 \times 16 \times 8$. The models are evaluated using various metrics, including PSNR, SSIM, LPIPS, and FVD, which are commonly used to assess the quality of reconstructions and generative performance. From the table, we can observe that OneVAE consistently outperforms other discrete-only and continuous-only models in most metrics. In summary, the quantitative results demonstrate that our OneVAE not only unifies discrete and continuous representations but also achieves superior overall reconstruction performance, further corroborating that discrete and continuous representations can be unified.

Method	Compression	z_dim	Unified Model	Token Type	PSNR (\uparrow)	SSIM (\uparrow)	LPIPS (\downarrow)	FVD (\downarrow)
CV-VAE		4	\times		31.12	0.9142	0.0554	100.72
Open-Sora-Plan-v1.2	$8 \times 8 \times 4$	4	\times		27.88	0.8840	0.0641	124.66
Open-Sora-v1.2		4	\times	Continuous	31.67	0.9147	0.0648	104.48
OneVAE		6	\checkmark		32.48	0.9335	0.0430	59.16
Cosmos Tokenizer	$16 \times 16 \times 4$		\times		30.61	0.9144	0.0739	135.68
Cosmos Tokenizer	$16 \times 16 \times 8$	16	\times	Continuous	29.98	0.9041	0.0868	154.34
OneVAE	$16 \times 16 \times 4$		\checkmark		32.43	0.9318	0.0535	87.61
OmniTokenizer			\times		23.73	0.8974	0.0735	206.18
Emu-3	$8 \times 8 \times 4$	-	\times		29.45	0.8912	0.0584	225.46
Cosmos Tokenizer			\times	Discrete	30.34	0.9159	0.0524	82.86
OneVAE			\checkmark		30.67	0.9228	0.0528	108.93
OneVAE-MT	$8 \times 8 \times 8$		\times		31.80	0.9399	0.0450	78.35
Cosmos Tokenizer	$8 \times 8 \times 8$		\times		27.17	0.8638	0.1409	303.37
Cosmos Tokenizer	$16 \times 16 \times 4$	-	\times	Discrete	26.80	0.8531	0.1260	350.87
Cosmos Tokenizer	$16 \times 16 \times 8$		\times		26.18	0.8342	0.1337	396.97
OneVAE	$16 \times 16 \times 4$		\checkmark		27.40	0.8690	0.1063	336.48
OneVAE-FE	$16 \times 16 \times 4$		\times		28.11	0.8772	0.0814	213.04

Table 1 Quantitative comparisons of reconstruction quality with baselines on the Panda70M test set demonstrate that our approach outperforms previous tokenizers. OneVAE-MT and OneVAE-FE correspond to our proposed multi-token quantization and first-frame enhancement strategies, respectively, as detailed in Sec. 3.2. OneVAE-MT employs an $8 \times 8 \times 8$ compression ratio, as it quantizes each spatial position into two tokens.

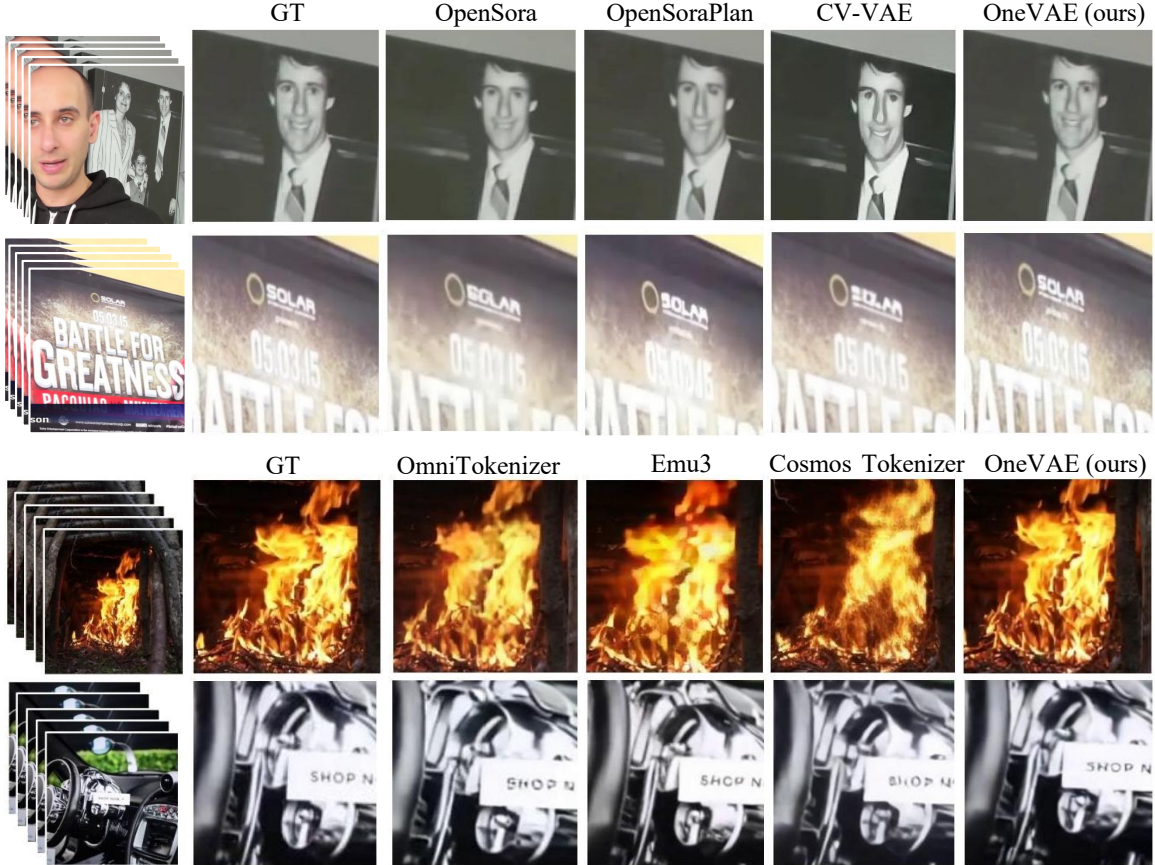


Figure 8 We present a qualitative comparison of our proposed unified model OneVAE with continuous only and discrete only methods, including CV-VAE [57], Open-Sora [59], Open-Sora-Plan [25], OmniTokenizer [45], and Emu-3 [46].

4.4 Qualitative Comparison

As shown in Fig. 8, we present a qualitative comparison of the performance of our proposed unified VAE (OneVAE) against several discrete-only and continuous-only baseline models under the closest model settings. When compared to continuous-only methods, it is evident that OneVAE produces the most accurate and high-fidelity reconstructions among all models. In the first example, our method reconstructs a clearer and more natural human face. In the second example, OneVAE successfully restores fine text details, demonstrating its superior capability in preserving structural integrity and texture clarity. When compared to discrete-only tokenizers, OneVAE again stands out by producing more realistic and visually appealing reconstructions. For the first video, OneVAE reconstructs richer and more detailed flames, whereas other methods produce blurry textures, especially struggling to preserve fine details. In the second comparison, OneVAE reconstructs sharper text, making it the only method among all comparisons that renders the text fully readable. Overall, despite as a unified discrete and continuous VAE, the qualitative results highlight that OneVAE reconstruct the most accurate and visually coherent videos, demonstrating its superior performance in preserving details and generating high-quality outputs.

5 Conclusions

In this work, we propose OneVAE, a unified VAE framework that bridges discrete and continuous video representations. By rethinking their connection, we propose a progressive training strategy leveraging pretrained continuous VAE priors, which accelerates convergence and improves performance. Furthermore, we propose a unified VAE that performs well on both discrete and continuous representations. To further enhance video VAE performance, we propose meaningful structural improvements: multi-token quantization to increase representational capacity, and first-frame enhancement to preserve anchor-frame fidelity in causal VAEs and improve temporal consistency. These designs significantly improve reconstruction quality under high compression. Extensive experiments validate that our approach achieves faster training, better reconstruction quality, and unified modeling capability—offering a promising direction for future video generation and video VAE.

References

- [1] Omer Bar-Tal, Hila Chefer, Omer Tov, Charles Herrmann, Roni Paiss, Shiran Zada, Ariel Ephrat, Junhwa Hur, Guanghui Liu, Amit Raj, et al. Lumiere: A space-time diffusion model for video generation. In *SIGGRAPH Asia 2024 Conference Papers*, pages 1–11, 2024. 4
- [2] Andreas Blattmann, Robin Rombach, Huan Ling, Tim Dockhorn, Seung Wook Kim, Sanja Fidler, and Karsten Kreis. Align your latents: High-resolution video synthesis with latent diffusion models. In *Proceedings of the IEEE/CVF conference on computer vision and pattern recognition*, pages 22563–22575, 2023. 3
- [3] Andrew Brock, Jeff Donahue, and Karen Simonyan. Large scale gan training for high fidelity natural image synthesis. *arXiv preprint arXiv:1809.11096*, 2018. 3
- [4] Tim Brooks, Bill Peebles, Connor Holmes, Will DePue, Yufei Guo, Li Jing, David Schnurr, Joe Taylor, Troy Luhman, Eric Luhman, Clarence Ng, Ricky Wang, and Aditya Ramesh. Video generation models as world simulators. 2024. 4
- [5] Ya-Liang Chang, Zhe Yu Liu, Kuan-Ying Lee, and Winston Hsu. Free-form video inpainting with 3d gated convolution and temporal patchgan. In *Proceedings of the IEEE/CVF international conference on computer vision*, 2019. 7
- [6] Junsong Chen, Jincheng Yu, Chongjian Ge, Lewei Yao, Enze Xie, Yue Wu, Zhongdao Wang, James Kwok, Ping Luo, Huchuan Lu, et al. Pixart-alpha: Fast training of diffusion transformer for photorealistic text-to-image synthesis. *arXiv preprint arXiv:2310.00426*, 2023. 2, 3
- [7] Liuhan Chen, Zongjian Li, Bin Lin, Bin Zhu, Qian Wang, Shenghai Yuan, Xing Zhou, Xinhua Cheng, and Li Yuan. Od-vae: An omni-dimensional video compressor for improving latent video diffusion model. *arXiv preprint arXiv:2409.01199*, 2024. 3
- [8] Tsai-Shien Chen, Aliaksandr Siarohin, Willi Menapace, Ekaterina Deyneka, Hsiang-wei Chao, Byung Eun Jeon, Yuwei Fang, Hsin-Ying Lee, Jian Ren, Ming-Hsuan Yang, et al. Panda-70m: Captioning 70m videos with multiple cross-modality teachers. In *Proceedings of the IEEE/CVF Conference on Computer Vision and Pattern Recognition*, pages 13320–13331, 2024. 7
- [9] Xiaokang Chen, Zhiyu Wu, Xingchao Liu, Zizheng Pan, Wen Liu, Zhenda Xie, Xingkai Yu, and Chong Ruan. Janus-pro: Unified multimodal understanding and generation with data and model scaling. *arXiv preprint arXiv:2501.17811*, 2025. 2

- [10] Patrick Esser, Sumith Kulal, Andreas Blattmann, Rahim Entezari, Jonas Müller, Harry Saini, Yam Levi, Dominik Lorenz, Axel Sauer, Frederic Boesel, et al. Scaling rectified flow transformers for high-resolution image synthesis. In *Forty-first international conference on machine learning*, 2024. 2, 3
- [11] Patrick Esser, Robin Rombach, and Bjorn Ommer. Taming transformers for high-resolution image synthesis. In *Proceedings of the IEEE/CVF conference on computer vision and pattern recognition*, pages 12873–12883, 2021. 2, 3, 4, 5
- [12] Songwei Ge, Thomas Hayes, Harry Yang, Xi Yin, Guan Pang, David Jacobs, Jia-Bin Huang, and Devi Parikh. Long video generation with time-agnostic vqgan and time-sensitive transformer. In *European Conference on Computer Vision*, pages 102–118. Springer, 2022. 3
- [13] Ian Goodfellow, Jean Pouget-Abadie, Mehdi Mirza, Bing Xu, David Warde-Farley, Sherjil Ozair, Aaron Courville, and Yoshua Bengio. Generative adversarial nets. *Advances in neural information processing systems*, 27, 2014. 3
- [14] Jonathan Ho, Ajay Jain, and Pieter Abbeel. Denoising diffusion probabilistic models. *Advances in neural information processing systems*, 33:6840–6851, 2020. 3
- [15] Jonathan Ho, Tim Salimans, Alexey Gritsenko, William Chan, Mohammad Norouzi, and David J Fleet. Video diffusion models. *Advances in Neural Information Processing Systems*, 35:8633–8646, 2022. 4
- [16] Junpeng Jiang, Gangyi Hong, Lijun Zhou, Enhui Ma, Hengtong Hu, Xia Zhou, Jie Xiang, Fan Liu, Kaicheng Yu, Haiyang Sun, et al. Dive: Dit-based video generation with enhanced control. *arXiv preprint arXiv:2409.01595*, 2024. 4
- [17] Yang Jin, Zhicheng Sun, Kun Xu, Liwei Chen, Hao Jiang, Quzhe Huang, Chengru Song, Yuliang Liu, Di Zhang, Yang Song, et al. Video-lavit: Unified video-language pre-training with decoupled visual-motional tokenization. *arXiv preprint arXiv:2402.03161*, 2024. 3
- [18] Tero Karras, Samuli Laine, and Timo Aila. A style-based generator architecture for generative adversarial networks. In *Proceedings of the IEEE/CVF conference on computer vision and pattern recognition*, pages 4401–4410, 2019. 3
- [19] Diederik P Kingma, Max Welling, et al. Auto-encoding variational bayes, 2013. 4
- [20] Weijie Kong, Qi Tian, Zijian Zhang, Rox Min, Zuozhuo Dai, Jin Zhou, Jiangfeng Xiong, Xin Li, Bo Wu, Jianwei Zhang, et al. Hunyuanvideo: A systematic framework for large video generative models. *arXiv preprint arXiv:2412.03603*, 2024. 2, 4, 5
- [21] PKU-Yuan Lab and Tuzhan AI etc. Open-sora-plan, April 2024. 4
- [22] Muyang Li, Ji Lin, Chenlin Meng, Stefano Ermon, Song Han, and Jun-Yan Zhu. Efficient spatially sparse inference for conditional gans and diffusion models. *Advances in neural information processing systems*, 35:28858–28873, 2022. 3
- [23] Tianhong Li, Yonglong Tian, He Li, Mingyang Deng, and Kaiming He. Autoregressive image generation without vector quantization. *Advances in Neural Information Processing Systems*, 37:56424–56445, 2024. 2
- [24] Zongjian Li, Bin Lin, Yang Ye, Liuhan Chen, Xinhua Cheng, Shenghai Yuan, and Li Yuan. Wf-vae: Enhancing video vae by wavelet-driven energy flow for latent video diffusion model. *arXiv preprint arXiv:2411.17459*, 2024. 4
- [25] Bin Lin, Yunyang Ge, Xinhua Cheng, Zongjian Li, Bin Zhu, Shaodong Wang, Xianyi He, Yang Ye, Shenghai Yuan, Liuhan Chen, et al. Open-sora plan: Open-source large video generation model. *arXiv preprint arXiv:2412.00131*, 2024. 5, 7, 8, 9
- [26] Ilya Loshchilov and Frank Hutter. Decoupled weight decay regularization. *arXiv preprint arXiv:1711.05101*, 2017. 7
- [27] Guoqing Ma, Haoyang Huang, Kun Yan, Liangyu Chen, Nan Duan, Shengming Yin, Changyi Wan, Ranchen Ming, Xiaoni Song, Xing Chen, et al. Step-video-t2v technical report: The practice, challenges, and future of video foundation model. *arXiv preprint arXiv:2502.10248*, 2025. 2
- [28] Fabian Mentzer, David Minnen, Eirikur Agustsson, and Michael Tschannen. Finite scalar quantization: Vq-vae made simple. *arXiv preprint arXiv:2309.15505*, 2023. 2, 3, 4, 7
- [29] NVIDIA. Cosmos tokenizer: A suite of image and video neural tokenizers, November 2024. 1, 2, 3, 4, 6, 8
- [30] Dustin Podell, Zion English, Kyle Lacey, Andreas Blattmann, Tim Dockhorn, Jonas Müller, Joe Penna, and Robin Rombach. Sdxl: Improving latent diffusion models for high-resolution image synthesis. *arXiv preprint arXiv:2307.01952*, 2023. 2, 3
- [31] Alec Radford, Karthik Narasimhan, Tim Salimans, Ilya Sutskever, et al. Improving language understanding by generative pre-training. 2018. 3
- [32] Aditya Ramesh, Prafulla Dhariwal, Alex Nichol, Casey Chu, and Mark Chen. Hierarchical text-conditional image generation with clip latents. *arXiv preprint arXiv:2204.06125*, 1(2):3, 2022. 3
- [33] Aditya Ramesh, Mikhail Pavlov, Gabriel Goh, Scott Gray, Chelsea Voss, Alec Radford, Mark Chen, and Ilya Sutskever. Zero-shot text-to-image generation. In *International conference on machine learning*, pages 8821–8831. Pmlr, 2021. 3

- [34] Robin Rombach, Andreas Blattmann, Dominik Lorenz, Patrick Esser, and Björn Ommer. High-resolution image synthesis with latent diffusion models. In *Proceedings of the IEEE/CVF conference on computer vision and pattern recognition*, pages 10684–10695, 2022. 1, 3, 4
- [35] Chitwan Saharia, William Chan, Saurabh Saxena, Lala Li, Jay Whang, Emily L Denton, Kamyar Ghasemipour, Raphael Gontijo Lopes, Burcu Karagol Ayan, Tim Salimans, et al. Photorealistic text-to-image diffusion models with deep language understanding. *Advances in neural information processing systems*, 35:36479–36494, 2022. 3
- [36] Fengyuan Shi, Zhuoyan Luo, Yixiao Ge, Yujiu Yang, Ying Shan, and Limin Wang. Taming scalable visual tokenizer for autoregressive image generation. *arXiv preprint arXiv:2412.02692*, 2024. 3, 4, 7
- [37] Uriel Singer, Adam Polyak, Thomas Hayes, Xi Yin, Jie An, Songyang Zhang, Qiyuan Hu, Harry Yang, Oron Ashual, Oran Gafni, et al. Make-a-video: Text-to-video generation without text-video data. *arXiv preprint arXiv:2209.14792*, 2022. 3, 4
- [38] Peize Sun, Yi Jiang, Shoufa Chen, Shilong Zhang, Bingyue Peng, Ping Luo, and Zehuan Yuan. Autoregressive model beats diffusion: Llama for scalable image generation. *arXiv preprint arXiv:2406.06525*, 2024. 1, 2
- [39] Anni Tang, Tianyu He, Junliang Guo, Xinle Cheng, Li Song, and Jiang Bian. Vidtok: A versatile and open-source video tokenizer. *arXiv preprint arXiv:2412.13061*, 2024. 3, 6
- [40] Chameleon Team. Chameleon: Mixed-modal early-fusion foundation models. *arXiv preprint arXiv:2405.09818*, 2024. 2
- [41] Thomas Unterthiner, Sjoerd Van Steenkiste, Karol Kurach, Raphaël Marinier, Marcin Michalski, and Sylvain Gelly. Fvd: A new metric for video generation. 2019. 7
- [42] Aaron Van Den Oord, Oriol Vinyals, et al. Neural discrete representation learning. *Advances in neural information processing systems*, 30, 2017. 3
- [43] Team Wan, Ang Wang, Baole Ai, Bin Wen, Chaojie Mao, Chen-Wei Xie, Di Chen, Feiwu Yu, Haiming Zhao, Jianxiao Yang, et al. Wan: Open and advanced large-scale video generative models. *arXiv preprint arXiv:2503.20314*, 2025. 2, 5
- [44] Jiuniu Wang, Hangjie Yuan, Dayou Chen, Yingya Zhang, Xiang Wang, and Shiwei Zhang. Modelscope text-to-video technical report. *arXiv preprint arXiv:2308.06571*, 2023. 3
- [45] Junke Wang, Yi Jiang, Zehuan Yuan, Bingyue Peng, Zuxuan Wu, and Yu-Gang Jiang. Omnitokenizer: A joint image-video tokenizer for visual generation. *Advances in Neural Information Processing Systems*, 37:28281–28295, 2024. 2, 3, 8, 9
- [46] Xinlong Wang, Xiaosong Zhang, Zhengxiong Luo, Quan Sun, Yufeng Cui, Jinsheng Wang, Fan Zhang, Yueze Wang, Zhen Li, Qiyang Yu, et al. Emu3: Next-token prediction is all you need. *arXiv preprint arXiv:2409.18869*, 2024. 1, 2, 8, 9
- [47] Yuqing Wang, Tianwei Xiong, Daquan Zhou, Zhijie Lin, Yang Zhao, Bingyi Kang, Jiashi Feng, and Xihui Liu. Loong: Generating minute-level long videos with autoregressive language models. *arXiv preprint arXiv:2410.02757*, 2024. 6
- [48] Zhou Wang, Alan C Bovik, Hamid R Sheikh, and Eero P Simoncelli. Image quality assessment: from error visibility to structural similarity. *IEEE transactions on image processing*, 2004. 7
- [49] Jay Zhangjie Wu, Yixiao Ge, Xintao Wang, Stan Weixian Lei, Yuchao Gu, Yufei Shi, Wynne Hsu, Ying Shan, Xiaoju Qie, and Mike Zheng Shou. Tune-a-video: One-shot tuning of image diffusion models for text-to-video generation. In *Proceedings of the IEEE/CVF International Conference on Computer Vision*, pages 7623–7633, 2023. 4
- [50] Wilson Yan, Matei Zaharia, Volodymyr Mnih, Pieter Abbeel, Aleksandra Faust, and Hao Liu. Elastictok: Adaptive tokenization for image and video. *arXiv preprint arXiv:2410.08368*, 2024. 3
- [51] Wilson Yan, Yunzhi Zhang, Pieter Abbeel, and Aravind Srinivas. Videogpt: Video generation using vq-vae and transformers. *arXiv preprint arXiv:2104.10157*, 2021. 2, 3
- [52] Zhuoyi Yang, Jiayan Teng, Wendi Zheng, Ming Ding, Shiyu Huang, Jiazheng Xu, Yuanming Yang, Wenyi Hong, Xiaohan Zhang, Guanyu Feng, et al. Cogvideox: Text-to-video diffusion models with an expert transformer. *arXiv preprint arXiv:2408.06072*, 2024. 2, 3, 4
- [53] Jiahui Yu, Yuanzhong Xu, Jing Yu Koh, Thang Luong, Gunjan Baid, Zirui Wang, Vijay Vasudevan, Alexander Ku, Yinfei Yang, Burcu Karagol Ayan, et al. Scaling autoregressive models for content-rich text-to-image generation. *arXiv preprint arXiv:2206.10789*, 2(3):5, 2022. 3
- [54] Lijun Yu, Yong Cheng, Kihyuk Sohn, José Lezama, Han Zhang, Huiwen Chang, Alexander G Hauptmann, Ming-Hsuan Yang, Yuan Hao, Irfan Essa, et al. Magvit: Masked generative video transformer. In *Proceedings of the IEEE/CVF Conference on Computer Vision and Pattern Recognition*, pages 10459–10469, 2023. 3
- [55] Lijun Yu, José Lezama, Nitesh B Gundavarapu, Luca Versari, Kihyuk Sohn, David Minnen, Yong Cheng, Vighnesh Birodkar, Agrim Gupta, Xiuye Gu, et al. Language model beats diffusion—tokenizer is key to visual generation. *arXiv preprint arXiv:2310.05737*, 2023. 1, 3

- [56] Richard Zhang, Phillip Isola, Alexei A Efros, Eli Shechtman, and Oliver Wang. The unreasonable effectiveness of deep features as a perceptual metric. In *Proceedings of the IEEE conference on computer vision and pattern recognition*, pages 586–595, 2018. 7
- [57] Sijie Zhao, Yong Zhang, Xiaodong Cun, Shaoshu Yang, Muyao Niu, Xiaoyu Li, Wenbo Hu, and Ying Shan. Cv-vae: A compatible video vae for latent generative video models. *arXiv preprint arXiv:2405.20279*, 2024. 1, 3, 4, 7, 8, 9
- [58] Chuanxia Zheng and Andrea Vedaldi. Online clustered codebook. In *Proceedings of the IEEE/CVF International Conference on Computer Vision*, pages 22798–22807, 2023. 3
- [59] Zangwei Zheng, Xiangyu Peng, Tianji Yang, Chenhui Shen, Shenggui Li, Hongxin Liu, Yukun Zhou, Tianyi Li, and Yang You. Open-sora: Democratizing efficient video production for all, March 2024. 4, 5, 8, 9
- [60] Yongxin Zhu, Bocheng Li, Yifei Xin, and Linli Xu. Addressing representation collapse in vector quantized models with one linear layer. *arXiv preprint arXiv:2411.02038*, 2024. 7